

# Kinetics of Pressure Dissolution of Enargite in Sulfate-Oxygen Media

R. PADILLA, C.A. RIVAS, and M.C. RUIZ

Enargite ( $\text{Cu}_3\text{AsS}_4$ ) is an increasingly common impurity in Chilean copper concentrates and its presence complicates the conventional treatment of the concentrates by smelting-converting because of the environmental risk of arsenic emissions to the atmosphere. Therefore, the recovery of copper from concentrates with high arsenic content must be carried out by non-conventional technologies. Sulfuric acid leaching processes are viable alternatives to treat copper concentrates with high content of enargite. Hence, in this article, the pressure leaching of enargite in the sulfuric acid-oxygen system is discussed. The leaching was studied at 160 °C to 220 °C and partial pressures of oxygen of 303 to 1013 kPa. The enargite dissolution was determined to occur as predicted by thermodynamics according to  $\text{Cu}_3\text{AsS}_4 + 8.75\text{O}_2 + 2.5\text{H}_2\text{O} + 2\text{H}^+ = 3\text{Cu}^{2+} + \text{H}_3\text{AsO}_4 + 4\text{HSO}_4^-$ . The leaching rate increased substantially with increasing temperature. Complete dissolution of enargite with particle size 64  $\mu\text{m}$  was obtained at 220 °C and 689 kPa of oxygen partial pressure in 120 minutes. The dissolution kinetics was analyzed by using the shrinking core model for spherical particles with surface chemical control. The rate of reaction was found to be 1/3 order with respect to the oxygen partial pressure and zero order with respect to sulfuric acid concentration. Activation energy of 69 kJ/mol was estimated for the dissolution reaction, which is a typical value for a chemically controlled process.

DOI: 10.1007/s11663-008-9151-9

© The Minerals, Metals & Materials Society and ASM International 2008

## I. INTRODUCTION

THE hydrometallurgical methods for extracting copper from concentrates are viable alternative processes especially when the concentrates contain appreciable amounts of toxic elements such as arsenic. In Chilean copper concentrates, arsenic is present mainly in the form of enargite ( $\text{Cu}_3\text{AsS}_4$ ), which is associated with most of the copper sulfides. When the enargite content in copper concentrates is relatively low, the concentrates are treated by conventional smelting-converting pyrometallurgical methods. However, if the concentrates contain appreciable amounts of enargite, the copper production by direct smelting and converting of the concentrate is problematical, because most of the arsenic reports to the gas phase increasing the risk of environmental pollution. In addition, the fraction of arsenic retained in the condensed metal phase leads to a deteriorated quality of the final metal product.<sup>[1–3]</sup> Thus, an additional step of pretreatment, such as roasting, may be required to eliminate arsenic from the concentrate prior to smelting when the arsenic content is over 2 pct.<sup>[3]</sup>

The natural alternative method to process copper concentrates with high enargite content is leaching. In particular, sulfuric acid leaching has always been considered as a viable process when direct smelting of

the concentrate is not technically feasible. The advantage of sulfuric acid leaching is that the pregnant solutions can be integrated to current solvent extraction and electrowinning operations. However, for a leaching process of copper concentrates to be effective, it is necessary to understand the leaching behavior not only of copper sulfides but also of the toxic impurities such as enargite present in the concentrate. In this framework, the present work is a kinetic study of the pressure leaching of enargite in sulfuric acid-oxygen media.

Recently, Lattanzi *et al.*<sup>[4]</sup> and Filippou *et al.*<sup>[5]</sup> reviewed the oxidation of enargite in various leaching media. Here, we briefly review the pertinent data on the aqueous oxidation of enargite in acidic solutions.

In 1952, Koch and Grasselly<sup>[6]</sup> studied the dissolution of enargite and enargite-pyrite mixtures in acidic ferric sulfate solutions. Their results indicated a very slow dissolution of enargite in this media and slightly accelerated dissolution in the presence of pyrite. Later in 1972, Dutrizac and MacDonald<sup>[7]</sup> studied the leaching kinetics of synthetic enargite discs in sulfuric acid-ferric sulfate solutions in the temperature range 60 °C to 95 °C. They also concluded that enargite dissolution was very slow in this leaching media and it occurred with linear kinetics. The sulfide sulfur was oxidized mainly to elemental sulfur, and the copper and arsenic concentrations in solution were close to stoichiometric proportions.

Hourn *et al.*<sup>[8]</sup> reported that an enargite-chalcocite ( $\text{Cu}_2\text{S}$ ) concentrate milled to a very fine size could be readily dissolved in an open reactor using a ferric ion-sulfuric acid lixiviant. More than 92 pct copper

---

R. PADILLA and M.C. RUIZ, Professors, Department of Metallurgical Engineering, and C.A. RIVAS, Student, Department of Chemical Engineering, are with the University of Concepción, Concepción, Chile. Contact e-mail: rpadilla@udec.cl

Manuscript submitted January 29, 2008.

Article published online June 13, 2008.

dissolution was achieved in 10 hours from a concentrate milled to 80 pct passing 3.5  $\mu\text{m}$ . The leaching conditions were 10 pct pulp density, 30 g/L ferric ions, 50 g/L sulfuric acid, 90 °C, oxygen sparging, and 2 kg/ton lignosol as sulfur dispersant.

Catalysts have also been used to accelerate the dissolution of enargite in leaching at atmospheric pressure. Flynn and Carnahan<sup>[9]</sup> found that by adding 0.25 g/L  $\text{Ag}_2\text{SO}_4$  in a lixiviant containing 0.8 mol/L  $\text{Fe}_2(\text{SO}_4)_3$  and 1 mol/L  $\text{H}_2\text{SO}_4$ , the dissolution of enargite reached 97 pct in 6 hours at the boiling point of the solution.

On the pressure leaching of enargite in sulfate media, Dreisinger and Saito<sup>[10]</sup> studied the total pressure oxidation of gold-rich enargite ore and concentrate from the El Indio mine (Barrick Corporation, Coquimbo Region, Chile). They found that at 220 °C and 689 kPa  $\text{O}_2$ , more than 95 pct of copper was extracted in 180 minutes and most of the dissolved arsenic reprecipitated as ferric arsenate.

Nadkarni and Kusik<sup>[11]</sup> leached enargite and mixtures of enargite-pyrite at about 225 °C and oxygen pressure of 1033 kPa. They reported 98 pct copper recovery in leaching enargite-pyrite mixtures and only 70 pct when pure enargite was leached. The beneficial effect of pyrite in the leaching was attributed to the generation of ferric ions in the system, which also contributed to the dissolution of enargite.

Regarding the dissolution of enargite in media other than sulfuric acid, Herreros *et al.*<sup>[12]</sup> studied the leaching in  $\text{Cl}_2/\text{HCl}$  solutions in the range 8 °C to 50 °C. They reported that after a very fast first reaction step (which lasted less than 30 seconds), a very slow second step followed with parabolic kinetics. The global stoichiometry of the leaching indicated that half of the sulfur in the enargite was oxidized to elemental sulfur and the other half to sulfate. Recently, Padilla *et al.*<sup>[13]</sup> studied the leaching of enargite in sulfate-chloride-oxygen system in the range 80 °C to 100 °C. These investigators found that the dissolution of enargite was also very slow in this media with only 6 pct of enargite dissolution in 7 hours at 100 °C. They reported that most of the sulfide sulfur oxidized to elemental sulfur, and the dissolution process was found to be surface reaction controlled with activation energy of 65 kJ/mol.

## II. THERMODYNAMICS OF THE $\text{Cu}_3\text{AsS}_4\text{-H}_2\text{SO}_4\text{-O}_2$ SYSTEM

Electrochemical phase diagrams ( $E_h$ -pH diagrams) are very useful to predict the stability or instability conditions of minerals in contact with aqueous solutions. For that reason, the  $E_h$ -pH diagrams for the  $\text{Cu}_3\text{AsS}_4\text{-H}_2\text{O}$  system at 25 °C and 200 °C were constructed considering the activities of the soluble species of Cu, As, and S equal to 0.1. The standard state chosen for all dissolved species was the hypothetical ideal solution of unit molality (1 mol of solute per kilogram of water). The thermodynamic data used in the construction of these equilibrium diagrams were obtained mainly from the HSC Chemistry database,<sup>[14]</sup> except for the Gibbs free energy values for enargite at 25 °C and 200 °C, which were calculated

from the measured heat capacity and entropy given by Seal II *et al.*<sup>[15]</sup> and the estimated heat of formation given by Knight.<sup>[16]</sup> The corresponding values are  $C_p^\circ = 196.7 + 4.99 \times 10^{-2} T - 1.918 \times 10^6 T^{-2}$  (J/K·mol),  $S_{298}^\circ = 257.75$  (J/mol), and  $\Delta H_{298}^\circ = 179.11$  (kJ/mol). In addition, the data for the arsenic species  $\text{HAsO}_3^{2-}$  and  $\text{AsO}_3^{3-}$  at 25 °C were taken from Dove and Rimstidt,<sup>[17]</sup> as shown in Table I. The average heat capacity of the ions in solution between 25 °C and 200 °C was estimated using the Criss and Cobble correlation<sup>[18]</sup> in HSC Chemistry.<sup>[14]</sup> Table I summarizes the standard free energy values of the various species used for the diagrams at 25 °C and 200 °C.

Figure 1 shows the equilibrium diagram of the  $\text{Cu}_3\text{AsS}_4\text{-H}_2\text{O}$  system at 25 °C. In this diagram, outside the area of stability of  $\text{Cu}_3\text{AsS}_4$ , the predominance areas for species pertaining to the S- $\text{H}_2\text{O}$  system and As- $\text{H}_2\text{O}$  system are also shown mainly to visualize the equilibrium products formed upon reaction of enargite with the aqueous media under different conditions of oxidation potential and pH. In this diagram, the S- $\text{H}_2\text{O}$  equilibria are shown using dashed lines and the As- $\text{H}_2\text{O}$  equilibria using short dashed lines. The limits of the stability region of water are also indicated using dash-dot lines.

The zone of interest in Figure 1 is the left upper corner of the diagram, corresponding to the acidic oxidizing conditions, which is the domain of the  $\text{Cu}^{2+}$  ions. It can be seen that in highly oxidizing conditions ( $E_h > 0.58$ ), the following soluble species will form on leaching enargite, depending on the pH of the solution.

**Table I. Standard Free Energy for the Various Species in the  $E_h$ -pH Diagrams**

Species	$\Delta G_{25^\circ\text{C}}^\circ$ (kJ/mol)	$\Delta G_{200^\circ\text{C}}^\circ$ (kJ/mol)
As	0.000	0.000
Cu	0.000	0.000
$\text{Cu}_3\text{AsS}_4$	-177.462	-174.359
$\text{CuH}_3$	283.576	289.333
$\text{CuO}$	-128.380	-112.273
$\text{Cu}_2\text{O}$	-147.982	-134.597
$\text{CuS}$	-53.507	-53.135
$\text{Cu}_2\text{S}$	-86.524	-90.493
S	0.000	0.000
$\text{AsH}_3$ (a)	80.642	94.701
$\text{Cu}^{2+}$ (a)	65.599	66.072
$\text{Cu}^+$ (a)	50.020	35.533
$\text{CuO}_2^{2-}$ (a)	-172.576	-77.598
$\text{H}_3\text{AsO}_3$ (a)	-640.061	-574.856
$\text{H}_2\text{AsO}_3^-$ (a)	-587.328	-506.519
$\text{HAsO}_3^{2-}$ (a)	-524.171	-401.154
$\text{AsO}_3^{3-}$	-447.577	-279.875
$\text{H}_3\text{AsO}_4$ (a)	-766.515	-685.283
$\text{H}_2\text{AsO}_4^-$ (a)	-753.620	-655.707
$\text{HAsO}_4^{2-}$ (a)	-714.942	-588.019
$\text{AsO}_4^{3-}$ (a)	-648.669	-482.181
$\text{H}_2\text{S}$ (a)	-27.281	-25.083
$\text{HS}^-$ (a)	12.087	35.496
$\text{S}^{2-}$ (a)	86.026	129.087
$\text{HSO}_4^-$ (a)	-756.182	-672.731
$\text{SO}_4^{2-}$ (a)	-744.865	-631.876

(a) refers to aqueous.

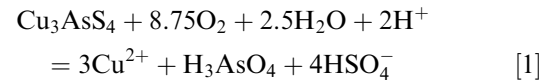
That is, at  $\text{pH} < 2$ , the predominant equilibrium species will be  $\text{Cu}^{2+}$ ,  $\text{H}_3\text{AsO}_4$ , and  $\text{HSO}_4^-$ ; at  $\text{pH}$  between 2 and 2.3, the predominant species will be  $\text{Cu}^{2+}$ ,  $\text{H}_3\text{AsO}_4$ , and  $\text{SO}_4^{2-}$ ; finally, at  $\text{pH}$  between 2.3 and 4.3,  $\text{Cu}^{2+}$ ,  $\text{H}_2\text{AsO}_4^-$ , and  $\text{SO}_4^{2-}$  will predominate. On the other hand, at lower oxidation potentials ( $E_h$  about 0.4 to 0.58), leaching of enargite can produce  $\text{Cu}^{2+}$ ,  $\text{H}_3\text{AsO}_3$ , and  $\text{HSO}_4^-$  for  $\text{pH} < 2$  or  $\text{Cu}^{2+}$ ,  $\text{H}_3\text{AsO}_3$ , and  $\text{SO}_4^{2-}$  for  $\text{pH} > 2$ .

The  $E_h$ - $\text{pH}$  equilibrium diagram for  $\text{Cu}_3\text{AsS}_4$ - $\text{H}_2\text{O}$  at 200 °C is shown in Figure 2. Similarly, in this diagram, the equilibria of the As- $\text{H}_2\text{O}$  and S- $\text{H}_2\text{O}$  systems and the limits of water stability are also shown. As can be seen, there are important differences between the 25 °C and 200 °C diagrams. The most significant changes are the appearance of stability fields for  $\text{Cu}^+$  and  $\text{CuO}_2^-$  at 200 °C. In addition, the equilibrium lines undergo a notorious change in position from 25 °C to 200 °C. For example, the predominance zone of  $\text{Cu}^{2+}$  at 25 °C

extends up to  $\text{pH} = 4.3$ , while at 200 °C, it extends only up to  $\text{pH} = 2.3$ . The  $\text{HSO}_4^-/\text{SO}_4^{2-}$  equilibrium shifts from  $\text{pH} = 2$  at 25 °C to 4.5 at 200 °C, and the  $\text{H}_3\text{AsO}_4/\text{H}_2\text{AsO}_4^-$  equilibrium shifts from  $\text{pH} = 2.3$  to 3.3. However, it should be pointed out that an increase in temperature will change the equilibrium solution speciation, thus altering the  $\text{pH}$ . In addition, due to the variation of water dissociation constant from  $1.02 \times 10^{-14}$  at 25 °C to  $4.84 \times 10^{-12}$  at 200 °C, the  $\text{pH}$  of neutrality at 200 °C will be 5.67 instead of 7.0.

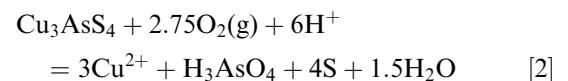
In Figure 2, we can also see that the predominant soluble products at 200 °C would be  $\text{Cu}^{2+}$ ,  $\text{H}_3\text{AsO}_4$ , and  $\text{HSO}_4^-$  at oxidation potentials over 0.45 V, while at lower oxidation potentials, in the range 0.38 to 0.45 V, the predominant species would be  $\text{Cu}^{2+}$ ,  $\text{H}_3\text{AsO}_3$ , and  $\text{HSO}_4^-$ .

Notwithstanding their differences, if the leaching of enargite is carried out in sufficiently acid conditions using oxygen as the oxidant, the two  $E_h$ - $\text{pH}$  diagrams discussed previously predict that enargite should dissolve at both 25 °C and 200 °C according to the following reaction:



The  $\text{H}_3\text{AsO}_4$  and  $\text{HSO}_4^-$  shown in this reaction are the predominant species of arsenic and sulfur formed at high acidic conditions. However, depending on the specific  $\text{pH}$  of the solution, a fraction of the arsenic and sulfur can also be present as  $\text{H}_2\text{AsO}_4^-$  and  $\text{SO}_4^{2-}$ , respectively. Reaction [1] is thermodynamically very favorable, with a standard free energy of  $-2821.8$  kJ/mol at 25 °C and  $-2476.7$  kJ/mol at 200 °C. However, despite the large negative free energy values (particularly at 25 °C), Reaction [1] does not occur at atmospheric conditions even at 100 °C.<sup>[13]</sup>

In practice, elemental sulfur has been observed to form instead of sulfate in the leaching of most sulfide minerals (including enargite) even at oxidation potentials far above the limits of its stability region.<sup>[12,19,20]</sup> Therefore, metastable elemental sulfur can also be formed instead of  $\text{HSO}_4^-$  (or  $\text{SO}_4^{2-}$ ) during the leaching of enargite with oxygen in acid media, especially in the lower temperature range. Thus, the following alternative reaction should be considered for the leaching of enargite.



The standard free energy values for this reaction are  $-747.7$  kJ/mol and  $-627.4$  kJ/mol at 25 °C and 200 °C, respectively, which are considerably less negative compared to the values of Reaction [1]. Nevertheless, Reaction [2] has been found to be the dominant reaction that occurs during the leaching of enargite in  $\text{H}_2\text{SO}_4$ - $\text{NaCl}$ - $\text{O}_2$  media at ambient pressure and temperatures in the range of 80 °C to 100 °C.<sup>[13]</sup> This reaction can also be expected to occur to a certain extent in the oxygen pressure leaching of enargite, especially in the lower temperature range considered in this research.

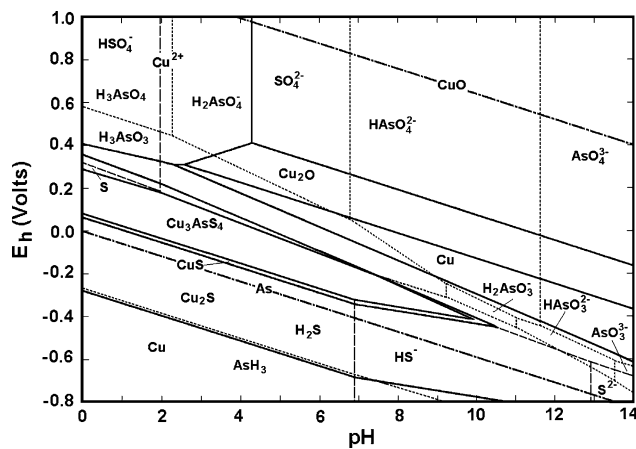


Fig. 1— $E_h$ - $\text{pH}$  diagram of the  $\text{Cu}_3\text{AsS}_4$ - $\text{H}_2\text{O}$  system at 25 °C for activities of soluble species of Cu, As, and S equal to 0.1. In the figure, S- $\text{H}_2\text{O}$  equilibria are shown as dashed lines and As- $\text{H}_2\text{O}$  equilibria as short dashed lines.

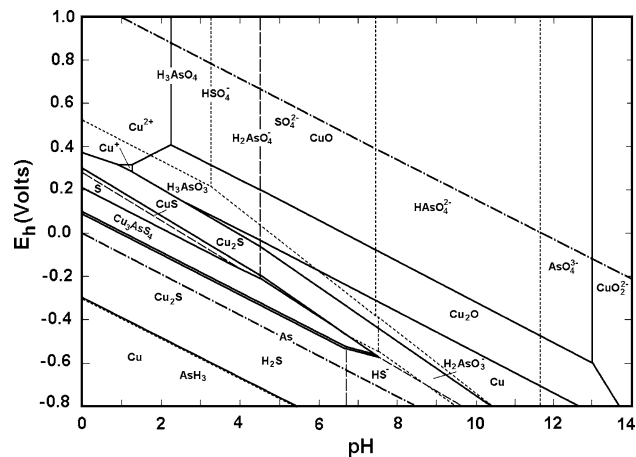


Fig. 2— $E_h$ - $\text{pH}$  diagram of the  $\text{Cu}_3\text{AsS}_4$ - $\text{H}_2\text{O}$  system at 200 °C for activities of soluble species of Cu, As, and S equal to 0.1. In the figure, S- $\text{H}_2\text{O}$  equilibria are shown as dashed lines and As- $\text{H}_2\text{O}$  equilibria as short dashed lines.

### III. EXPERIMENTAL METHOD

#### A. Materials

High-grade enargite mineral samples were obtained from El Indio Mine. Pure enargite crystals were selected for the experimental study, which were crushed, ground, and classified into size fractions using a U.S. sieve series with a ratio of the aperture widths of adjacent sieves equal to  $\sqrt{2}$ . The average size of each size fraction was calculated as the arithmetic mean of the corresponding aperture widths. The chemical analysis for the size fractions 150/106  $\mu\text{m}$  (average size 128  $\mu\text{m}$ ) and 53/38  $\mu\text{m}$  (average size 46  $\mu\text{m}$ ) is shown in Table II. These results indicate that the two size fraction samples had the same composition, as expected for a high-grade enargite sample. The mineralogical composition of the 46- $\mu\text{m}$  average size fraction sample is summarized in Table III. We can observe that the major constituent species for the prepared sample were enargite and gangue minerals with very little covellite and a negligible amount of pyrite.

The enargite sample was also characterized by X-ray diffraction (XRD) analysis. The results showed only diffraction lines for enargite ( $\text{Cu}_3\text{AsS}_4$ ), as expected. The gangue components did not appear in the pattern most likely because of their low concentration in the enargite sample.

#### B. Leaching Experiments

Experiments on pressure oxidation of enargite were carried out in a 1.5-L Parr titanium autoclave equipped with a proportional-integral-derivative temperature controller and ancillary system to provide oxygen overpressure. The autoclave had a variable speed stirrer with two axial impellers mounted 34 mm apart and a liquid sampling system. This autoclave was also equipped with an internally mounted cooling coil and an external electric heating system.

The experimental procedure consisted of charging the autoclave with 1 L of  $\text{H}_2\text{SO}_4$  solution, which was preheated to about 95 °C. Once at this temperature, 2 g of enargite sample were added and the autoclave was sealed and heated to the temperature specified for the

Table II. Chemical Analysis of Enargite Samples

Average Particle Size Fraction, $\mu\text{m}$	Pct Cu	Pct S	Pct As
128	45.39	31.70	18.95
46	45.35	31.56	18.90

Table III. Mineralogical Composition of Enargite Sample of Average Size Fraction of 46  $\mu\text{m}$

Mineral	Content (Mass Pct)
Enargite	93.54
Covellite	0.4
Pyrite	0.06
Gangue minerals	6.0

test. The oxygen was introduced, the pressure was then fixed to the desired value, and the system was allowed to react. During the experiment, various liquid samples were withdrawn from the reactor at specified times, and at the end of the experiment, the autoclave was rapidly cooled by circulating cold water through the cooling coil, and the solid residues were filtered, washed with acidified water, and dried overnight at 65 °C. The withdrawn liquid samples and the final filtrate were analyzed for copper and, in some cases, for arsenic by atomic absorption spectroscopy.

### IV. RESULTS

#### A. Preliminary Experiments

The main variables expected to have some influence on the dissolution rate of enargite were stirring speed, concentration of sulfuric acid, temperature, partial pressure of oxygen, and particle size of the sample. In order to determine the appropriate conditions in which enargite can be leached, various preliminary leaching experiments were conducted, which showed that enargite can be dissolved at appreciable rates only above 160 °C. At lower temperatures, the dissolution rate was slow even for oxygen partial pressures up to 1519 kPa.

Additionally, preliminary experiments conducted at 200 °C and 1013 kPa of oxygen overpressures, as illustrated in Figure 3, showed similar extraction of copper and arsenic, indicating that the enargite dissolution is close to stoichiometric proportions within the experimental error of analysis. This result was anticipated because stoichiometric dissolution of enargite has been reported previously.<sup>[7]</sup> Therefore, the fraction of enargite dissolution can be calculated by following the changes in either copper or arsenic concentration in the solution. In this research, by convenience, the dissolution of enargite was followed by the determination of

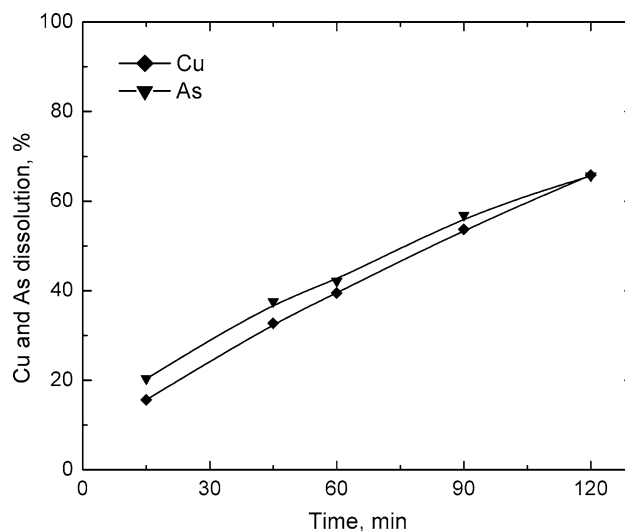


Fig. 3—Copper and arsenic dissolution from enargite sample with particle size of 128  $\mu\text{m}$ , 800 rpm, 0.2 m  $\text{H}_2\text{SO}_4$ , 1013 kPa of oxygen partial pressure, and 200 °C.



copper in solution. The reproducibility of our experimental sampling system was also checked and found to be acceptable within the limits of analytical error.

### B. Characterization of the Solid Residues from Leaching

The solid residues from some leaching experiments were analyzed by XRD for identification of reaction products. Figure 4 shows the diffraction pattern for nonreacted enargite sample and the pattern for a residue obtained in leaching for 150 minutes at 200 °C and 689 kPa of oxygen overpressure with about 90 pct of copper extracted. The XRD pattern of the residue is the same as that obtained for unreacted enargite, indicating that the dissolution of enargite proceeds without the formation of elemental sulfur or intermediate solid products at 200 °C. Some solid residues were also analyzed for elemental sulfur by extracting the sulfur with carbon disulfide (CS<sub>2</sub>) in a Soxhlet extractor. In this method, the solvent CS<sub>2</sub> is recycled by evaporation and condensation and the condensed solvent is used repeatedly to extract the elemental sulfur from the residue held in a narrow thimble constructed of heavy filter paper.<sup>[21]</sup> Once the extraction has been completed, the solvent is evaporated to yield the dissolved elemental sulfur. This method detected a small amount of elemental sulfur in the residue obtained at the lowest temperature (160 °C), equivalent to 8 pct of the sulfide sulfur in the enargite. At the higher temperatures, elemental sulfur was not found in the residues. These results indicate that Reaction [1] is the dominant reaction occurring during the pressure leaching of enargite in the range of 160 °C to 220 °C, as predicted by thermodynamics.

### C. Effect of Agitation

The effect of stirring speed on the enargite dissolution was studied by leaching the sample with average particle size of 128 μm in 0.2 m (molal) H<sub>2</sub>SO<sub>4</sub> solution, at

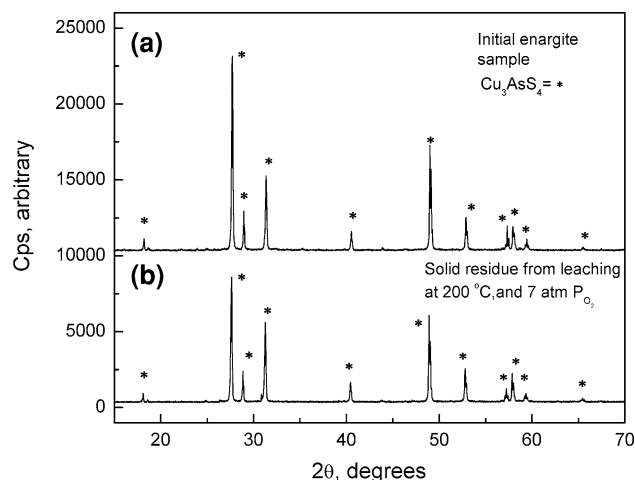


Fig. 4—X-ray diffraction pattern of (a) unreacted enargite sample compared to the pattern of (b) a residue from leaching at 689 kPa of oxygen overpressures and 200 °C.

oxygen partial pressure of 689 kPa and 200 °C. The results obtained in leaching for 60 and 120 minutes are shown in Figure 5. In both cases, agitation has a notorious effect on the copper dissolution up to about 600 rpm. At higher agitations, the copper dissolution does not change noticeably, indicating that over 600 rpm there is an adequate suspension of the solid particles and good distribution of oxygen in the solution. Therefore, most of the experiments were carried out at 800 rpm to assure independence of this variable.

### D. Effect of Concentration of Sulfuric Acid and Oxygen Partial Pressure

To study the influence of the initial sulfuric acid concentration on the rate of enargite dissolution, experiments were carried out with initial acid concentrations in the range 0.1 to 0.51 m (molal). The results shown in Figure 6 were obtained in leaching enargite of average size 128 μm at 200 °C, 689 kPa partial pressure of oxygen, and 120 minutes. In this figure, we can clearly see that the copper dissolution from enargite is affected by the initial acid concentration up to concentrations around 0.2 m. Concentrations over 0.2 m and up to 0.5 m do not have any further effect on the copper dissolution. This result was anticipated because the primary role of the acid in the leaching was to keep the copper ions in solution (preventing the hydrolysis of the Cu<sup>2+</sup> ions) and to protonate the arsenic(V) and sulfur(VI) products. On the other hand, the effect of oxygen overpressure on the copper dissolution was studied in the range 303 to 1013 kPa at 190 °C, and the results are shown in Figure 7. We can observe in this figure that the copper dissolution increases with an increase in the oxygen partial pressure from 303 to 1013 kPa; nevertheless, the rate dependence on the oxygen partial pressure of oxygen is not large.

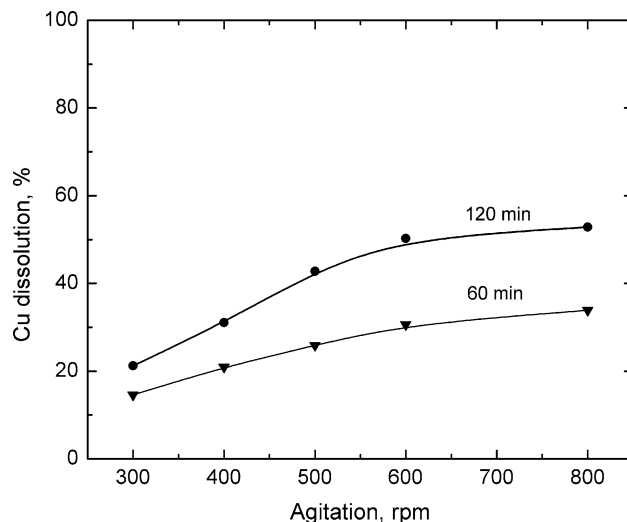


Fig. 5—Effect of agitation on the dissolution of enargite. Leaching conditions: enargite particle size 128 μm, 0.2 m H<sub>2</sub>SO<sub>4</sub>, 689 kPa of partial pressure of oxygen, and 200 °C for 60 and 120 min of leaching.

### E. Effect of Particle Size

Leaching experiments were carried out using four enargite size fractions: 150/106  $\mu\text{m}$ , 106/75  $\mu\text{m}$ , 75/53  $\mu\text{m}$ , and 53/38  $\mu\text{m}$ , with average sizes ranging from 46 to 128  $\mu\text{m}$ . The results are summarized in Figure 8, where we can see that the rate of copper dissolution increases when the initial size of the particle decreases. The decrease in the rate for large particles is probably due to the reduction of the interfacial area of reaction, because passivation is not apparent from the rate curves even for the largest particle size.

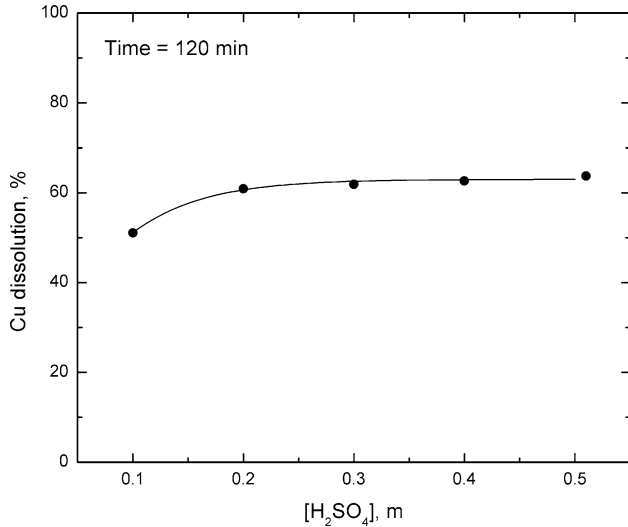


Fig. 6—Effect of initial sulfuric acid concentration on the dissolution of enargite. Leaching conditions: enargite particle size 128  $\mu\text{m}$ , 800 rpm, 689 kPa of partial pressure of oxygen, 200  $^{\circ}\text{C}$ , and 120 min of total time.

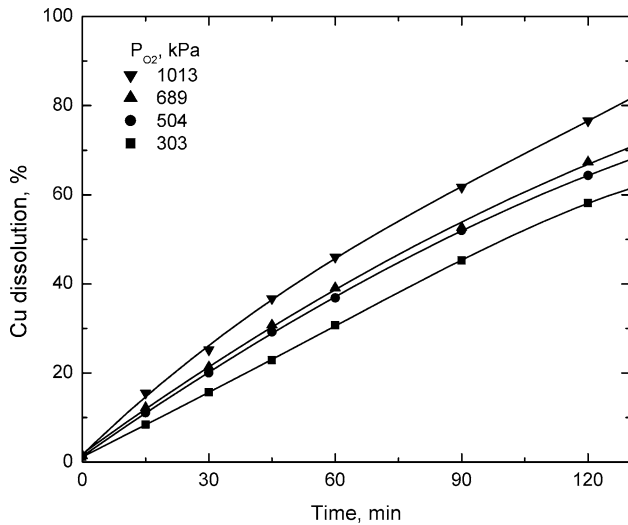


Fig. 7—Dissolution of enargite at various partial pressures of oxygen. Leaching conditions: enargite particle size 46  $\mu\text{m}$ , 800 rpm, 0.2 m  $\text{H}_2\text{SO}_4$ , and 190  $^{\circ}\text{C}$ .

### F. Effect of Temperature

Because the leaching rate was very slow at temperatures lower than 160  $^{\circ}\text{C}$ , the temperature was varied from 160  $^{\circ}\text{C}$  to 220  $^{\circ}\text{C}$  to determine the effect of this variable on the reaction rate. The other variables were kept constant at 689 kPa of oxygen overpressure, 0.2 m  $\text{H}_2\text{SO}_4$ , and 800 rpm stirring speed, and the initial average particle size of the sample was 64  $\mu\text{m}$ . The results are shown in Figure 9, where we can see that the temperature has an important effect on the leaching rate. For example, we can observe in this figure that a change in temperature from 160  $^{\circ}\text{C}$  to 220  $^{\circ}\text{C}$  produced an increase in the dissolution of enargite from about 20 to 100 pct in 120 minutes. This large temperature

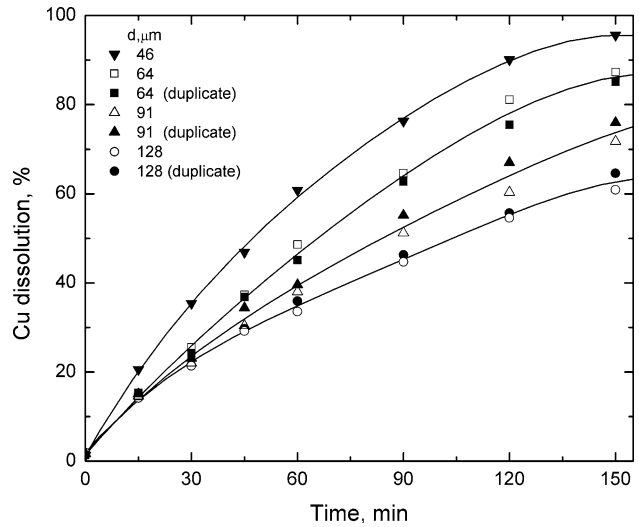


Fig. 8—Effect of initial particle size on the rate of enargite dissolution in pressure leaching at 200  $^{\circ}\text{C}$  and 689 kPa of partial pressure of oxygen: 800 rpm and 0.2 m  $\text{H}_2\text{SO}_4$ .

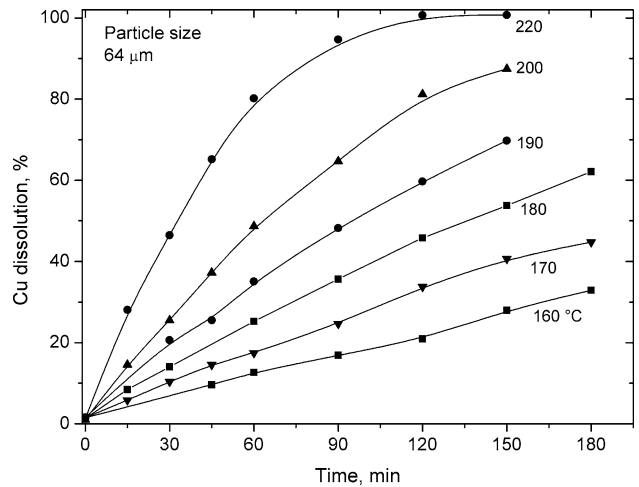


Fig. 9—Dissolution of enargite at various temperatures. Leaching conditions: enargite particle size 64  $\mu\text{m}$ , 800 rpm, 0.2 m  $\text{H}_2\text{SO}_4$ , and partial pressure of oxygen 689 kPa.

dependence is typically found in leaching systems where the controlling step is a surface chemical reaction.

### G. Leaching Kinetics

The significant dependence of the enargite dissolution on temperature suggests that the controlling step is a surface chemical reaction. Therefore, assuming surface reaction control, the rate equation for a shrinking spherical enargite particle of initial radius  $r_0$  for constant concentration of the reactants can be written as<sup>[22]</sup>

$$1 - (1 - X)^{1/3} = kt \quad [3]$$

where  $X$  is the fraction of enargite reacted,  $t$  is the leaching time, and  $k$  is the global kinetic constant given by the following general expression:

$$k = \frac{k' C_{H^+}^p C_{O_2}^q}{r_0} \quad [4]$$

where  $k'$  is a rate constant;  $C_{O_2}$  and  $C_{H^+}$  are the solution concentration of oxygen and hydrogen ion, respectively; and  $p$  and  $q$  are the apparent reaction orders. Because the rate of dissolution becomes independent of the concentration of acid in the range used in this research ( $>0.2$  M), as shown in Figure 6, zero order of reaction can be assumed for the hydrogen ion concentration. On the other hand, the concentration of oxygen in the solution will be equal to the saturation solubility of oxygen, which for any given condition is proportional to the partial pressure of oxygen.<sup>[23]</sup> Therefore, the global rate constant can be expressed as

$$k = \frac{k_l P_{O_2}^q}{r_0} \quad [5]$$

where  $k_l$  is the linear rate constant and  $P_{O_2}$  is the partial pressure of oxygen.

Figure 10 shows a plot of  $1 - (1 - X)^{1/3}$  as a function of time for the experimental data obtained in the range 160 °C to 220 °C for enargite samples with average particle size of 64  $\mu\text{m}$ . We observe in this figure an excellent linear fit of the kinetic data with regression coefficients,  $R^2$ , for the six temperatures ranging from 0.992 to 0.998, indicating the applicability of Eq. [3]. The values of the global kinetic constants  $k$  at the various temperatures were obtained from the slopes of the straight lines.

For chemical-reaction-controlled kinetics,  $k$  should vary linearly with the inverse of initial particle radius, as indicated in Eq. [5]. In order to verify this dependence, the data concerning particle size (Figure 8) were fitted according to Eq. [3] and the result is shown in Figure 11. The  $k$  values obtained from this figure were plotted as a function of the inverse of the initial particle radius in Figure 12. The good linear dependency of the data shown in this figure ( $R^2 = 0.982$ ) supports the kinetic model used.

On the other hand, the reaction order  $q$  was calculated from the kinetic data on the effect of the partial pressure of oxygen. Figure 13 shows the experimental data for various partial pressures of oxygen

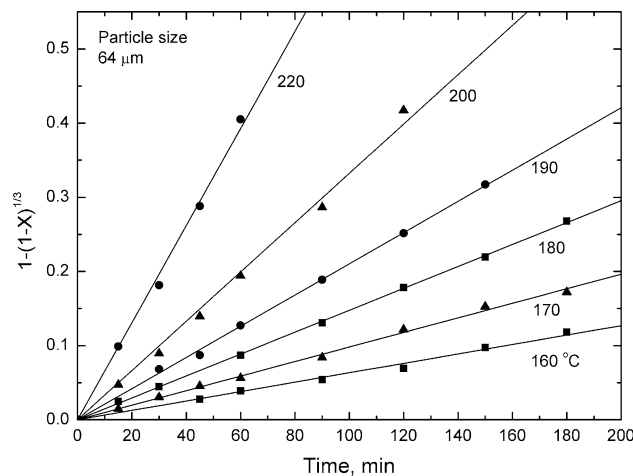


Fig. 10—Dissolution kinetics of enargite sample with average particle size of 64  $\mu\text{m}$  in pressure leaching with  $\text{H}_2\text{SO}_4\text{-O}_2$  media for the leaching conditions of Fig. 9.

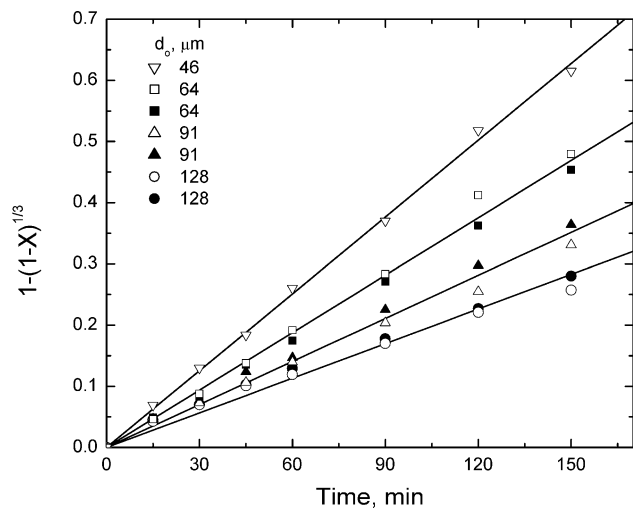


Fig. 11—Dissolution kinetics of enargite sample with various particle sizes in pressure leaching with  $\text{H}_2\text{SO}_4\text{-O}_2$  media for the conditions of Fig. 8.

plotted according to Eq. [3], and the  $k$  values obtained were used to draw a plot of logarithm of  $k$  vs the logarithm of  $p_{O_2}$ , as shown in Figure 14. The result is a linear relationship with  $R^2$  equal to 0.988 and a slope equal to 1/3. This fractional reaction order suggests that the kinetics of dissolution reaction occurs through a complex electrochemical mechanism, which was not elucidated in this research.

The calculated values of the kinetic constant  $k_l$  were used to draw an Arrhenius plot shown in Figure 15. One can observe in this figure an excellent linear fit ( $R^2 = 0.999$ ) of the temperature dependency of the linear kinetics constant. The calculated energy of activation was 69 kJ/mol for the temperature range of 160 °C to 220 °C, which is a typical value for a reaction occurring under chemical reaction control.

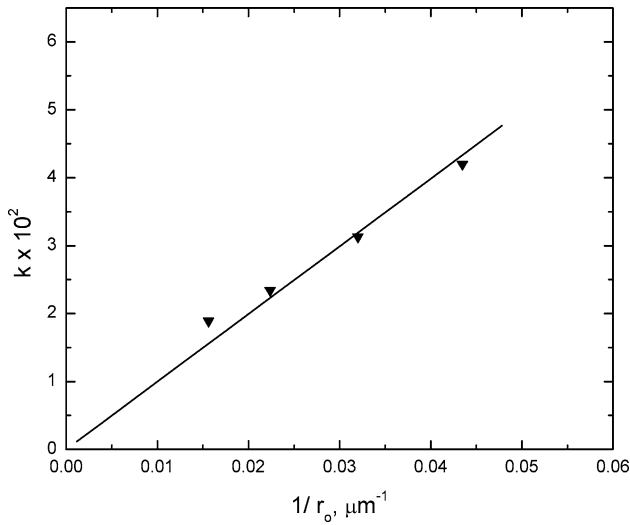


Fig. 12—Rate constant dependency on the inverse of initial particle size in pressure leaching of enargite in  $H_2SO_4-O_2$  media.

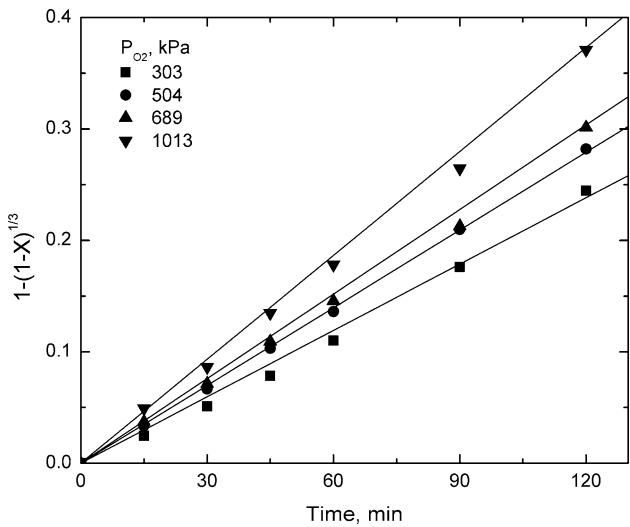


Fig. 13—Rate of enargite dissolution at various partial pressures of oxygen at  $190\text{ }^\circ\text{C}$  in  $H_2SO_4-O_2$  media for the leaching conditions of Fig. 7.

Thus, the kinetics of the pressure leaching of enargite in sulfuric acid–oxygen system can be represented by

$$1 - (1 - X)^{1/3} = \frac{5.09 \times 10^5 \cdot P_{O_2}^{1/3} \left[ \exp\left(\frac{-69,000}{RT}\right) \right]}{r_o} t \quad [6]$$

where  $R$  is equal to  $8.314\text{ J mol}^{-1}\text{ K}^{-1}$ ,  $r_o$  is in micrometers,  $P_{O_2}$  is in kPa,  $t$  is in minutes, and  $k_l = 5.09 \times 10^5\text{ }\mu\text{m}\cdot\text{kPa}^{-1/3}\cdot\text{min}^{-1}$ .

Overall, the present study has shown that enargite can be dissolved at fast rates at temperatures over  $200\text{ }^\circ\text{C}$  (high-temperature acid pressure leaching), indicating the feasibility of treating chalcopyritic concentrates with high enargite content. In such a case, the rate equation found in the present study may be affected by the presence of ferric ions in the solution and by possible

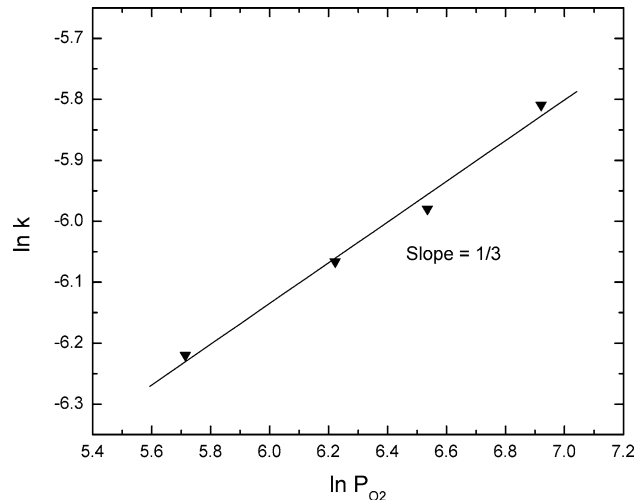


Fig. 14—Rate constant dependency on the partial pressure of oxygen in  $H_2SO_4-O_2$  media.

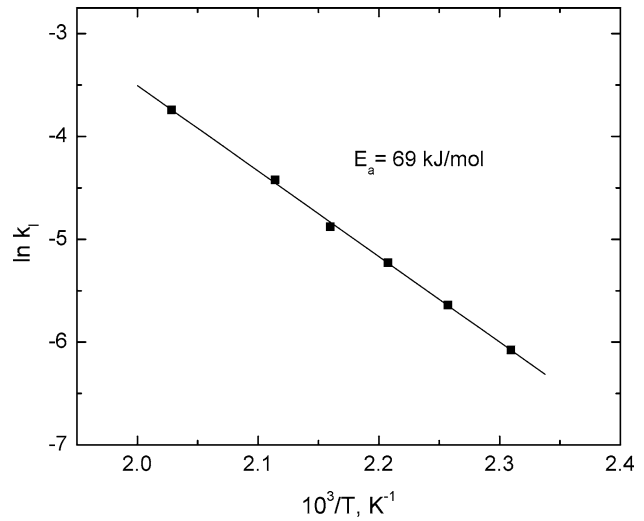
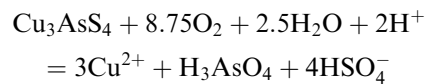


Fig. 15—Arrhenius plot for the pressure dissolution of enargite in sulfate-oxygen media.

galvanic interactions between the various minerals in the copper concentrate.

## V. CONCLUSIONS

The pressure leaching of enargite in the temperature range studied,  $160\text{ }^\circ\text{C}$  to  $220\text{ }^\circ\text{C}$ , occurs as predicted by thermodynamics according to



From the studied variables, temperature has the largest influence on the dissolution rate. Complete dissolution of enargite with particle size  $64\text{ }\mu\text{m}$  can be obtained at  $220\text{ }^\circ\text{C}$  and  $689\text{ kPa}$  of partial pressure of



oxygen and 120 minutes of leaching time. On the other hand, the concentration of sulfuric acid over 0.2 m has negligible effect on the dissolution rate, indicating a rate dependency on acid concentration of zero order.

The dissolution kinetics of enargite was analyzed by using the shrinking core kinetic expression for spherical particles with surface chemical control given by  $1 - (1 - X)^{1/3} = kt$ , with  $k = \frac{k_t P_{O_2}^n}{r_o}$ . This model represented the data well. The order of reaction with respect to the oxygen partial pressure was found to be 1/3, and the activation energy for the dissolution reaction was 69 kJ/mol, which is a typical value for a chemically controlled process.

### ACKNOWLEDGMENTS

The authors acknowledge The National Fund for Scientific and Technological Development, FONDECYT, of Chile for the financial support of this study through Project No. 1050948.

### REFERENCES

1. J.V. Wiertz and M. Gutiérrez: in *Environment & Innovation in Mining and Mineral Technology*, M.A. Sánchez, F. Vergara, and S.H. Castro, eds., University of Concepción, Concepción, Chile, 1998, pp. 593–602.
2. J.E. Hoffmann: *JOM*, 1993, vol. 45 (8), pp. 30–31.
3. N.L. Piret: *Proc. Copper 99-Cobre 99 Int. Conf., Vol. I—Mineral Processing/Environment, Health and Safety*, B.A. Hancock and M.R.L. Pon, eds., TMS, Warrendale, PA, 1999, pp. 321–40.

4. P. Lattanzi, S. Da Pelo, E. Musu, D. Atzei, B. Elsener, M. Fantauzzi, and A. Rossi: *Earth Sci. Rev.*, 2008, vol. 86, pp. 62–88.
5. D. Filippou, P. St-Germain, and T. Grammatikopoulos: *Miner. Process. Extract. Metall. Rev.*, 2007, vol. 28, pp. 247–98.
6. S. Koch and G. Grasselly: *Acta Miner. Petrogv. Szeged.*, 1952, vol. 6, pp. 23–29.
7. J.E. Dutrizac and R.J.C. MacDonald: *Can. Metall. Q.*, 1972, vol. 11 (3), pp. 469–76.
8. M.M. Hourn, D.W. Turner, and I.R. Holtzberger: U.S. Patent 5,993,635, Nov. 30, 1999.
9. C.M. Flynn Jr. and T.G. Carnahan: U.S. Patent 4,888,207, Dec. 19, 1989.
10. D.B. Dreisinger and B.R. Saito: *Proc. Copper 99-Cobre 99 Int. Conf., Vol. IV—Hydrometallurgy of Copper*, S.K. Young, D.B. Dreisinger, R.P. Hachl, and D.G. Dixon, eds., TMS, Warrendale, PA, 1999, pp. 181–95.
11. R.M. Nadkarni and C.L. Kusik: in *Arsenic Metallurgy: Fundamentals and Applications*, R.G. Reddy, J.L. Hendrix, and P.B. Queneau, eds., TMS, Warrendale, PA, 1988, pp. 263–86.
12. O. Herreros, R. Quiroz, M.C. Hernández, and J. Viñals: *Hydrometallurgy*, 2002, vol. 62, pp. 153–60.
13. R. Padilla, D. Girón, and M.C. Ruiz: *Hydrometallurgy*, 2005, vol. 80, pp. 272–79.
14. A. Roine: *HSC Chemistry 4.0*, Outokumpu Research Oy, Pori, Finland, 1999.
15. R.R. Seal II, R.A. Robie, B.S. Hemingway, and H.T. Evans, Jr.: *J. Chem. Thermodyn.*, 1996, vol. 28, pp. 406–12.
16. J.E. Knight: *Econ. Geol.*, 1977, vol. 72, pp. 1321–36.
17. P.M. Dove and J.D. Rimstidt: *Am. Mineral.*, 1985, vol. 70, pp. 838–44.
18. C.M. Criss and J.W. Cobble: *J. Am. Chem. Soc.*, 1964, vol. 86, pp. 5385–90.
19. E. Peters: *Metall. Trans. B*, 1976, vol. 7B, pp. 505–17.
20. R.G. MacDonald and D.M. Muir: *Hydrometallurgy*, 2007, vol. 86 (3–4), pp. 206–20.
21. W.E. Harris and B. Kratochvil: *An Introduction to Chemical Analysis*, Saunders College Publishing, Philadelphia, PA, 1981, pp. 463–64.
22. H.Y. Sohn and M.E. Wadsworth: *Rate Processes of Extractive Metallurgy*, Plenum Press, New York, NY, 1979, pp. 141–43.
23. D. Tromans: *Hydrometallurgy*, 1998, vol. 50, pp. 279–96.